Magnetic ordering in a (001) Sm layer and a Sm/Y superlattice studied by resonant x-ray magnetic scattering

2000 J. Phys.: Condens. Matter 12 3091

(http://iopscience.iop.org/0953-8984/12/13/317)

J. Phys.: Condens. Matter **12** (2000) 3091–3100. Printed in the UK PII: S0953-8984(00)09916-1

Magnetic ordering in a (001) Sm layer and a Sm/Y superlattice studied by resonant x-ray magnetic scattering

K Dumesnil†, C Dufour†, A Stunault‡ and Ph Mangin†

† Laboratoire de Physique des Matériaux, Université Henri Poincaré-Nancy 1, BP 239, 54506 Vandoeuvre les Nancy Cedex, France
‡ XMaS the UK CRG at ESRF, BP 220, 38043 Grenoble Cedex, France,
and
Department of Physics, University of Liverpool, Liverpool L69 7ZE, UK

Received 26 November 1999, in final form 26 January 2000

Abstract. The magnetic ordering of samarium in a 5000 Å thick (001) Sm film and in a (001) Sm/Y superlattice has been investigated using resonant x-ray magnetic scattering at the samarium L_3 edge. In both samples, the hexagonal sublattice orders below $T_N = 106$ K. Magnetic resonances of dipolar and quadrupolar origin are observed above and below the edge respectively and allow one to study the 5d and 4f magnetism separately. In the film, the cubic sublattice also shows long range magnetic order below 12 K. The relative contributions of the 4f and 5d electrons to the magnetic moments on the hexagonal sites are the same for $T < 12$ K, 12 K $< T < T_N$ and close to T_N. In the superlattice, the Y and Sm layers mainly retain their own bulk crystallographic structure (i.e. hcp and 'Sm structure' respectively). The hexagonal sublattice of the Sm layers shows the same magnetic structure as in the thick film, but the energy dependence of the resonance is different. There is no coherence of the magnetic structure through the Y spacer layers.

1. Introduction

Among the rare earths, bulk samarium presents an original crystal structure, referred to as the 'Sm structure' in the following. This structure is intermediate between the dhcp structure and the hcp one and consists of the periodic compact stacking of nine hexagonal planes along the $\boldsymbol{c}$-axis ($A_cB_hA_hB_cC_hB_hC_cA_hC_h\ldots$), leading to a c lattice constant of 26.21 Å at room temperature [1]. The h and c subscripts refer to the local symmetry—hexagonal or cubic—of the atoms in each basal plane. Because of the huge thermal neutron absorption cross section of natural samarium and the small value of the ordered magnetic moment (0.1 μ_B), the magnetic structure of bulk samarium was determined only in 1972 by neutron diffraction from an isotopically enriched sample [2]. The magnetic moments on the hexagonal sites order antiferromagnetically below $T_N = 106$ K. They point along the $\boldsymbol{c}$-axis and couple ferromagnetically in each basal plane with an antiferromagnetic arrangement along $\boldsymbol{c}$, in a (0++0−−0++0−− ...) sequence. The zeros correspond to the 'cubic planes', where the moments are still disordered. More recent resonant x-ray magnetic scattering (RXMS) results are consistent with this magnetic structure [3]. The cubic sublattice orders separately below 14 K in a more complex antiferromagnetic structure where the magnetic unit cell is four times the chemical one along the $\boldsymbol{c}$-axis and along one of the hexagonal $\boldsymbol{a}$-axes. These specific magnetic structures of samarium are caused by cooperating and competing oscillatory long-range coupling of the 4f moments via the conduction electron and crystal field effects.

0953-8984/00/133091+10$30.00

The Sm^{3+} free-ion moment is 0.71 μ_B, a rather small value resulting from spin and orbital moments of opposite directions. The value of 0.1 μ_B determined from the neutron study [2] is interpreted in terms of a large polarization of the conduction electrons parallel to the ionic spin, which almost cancels the orbital moment. However, a more recent neutron study performed on a 5000 Å thick samarium epitaxial film has resulted in a much larger value of 1.2 ± 0.2 μ_B [4].

Owing to the large enhancement of the magnetic scattering cross-sections close to the $L_{2,3}$ absorption edges of rare earths, RXMS is a powerful technique to investigate the magnetism of rare earth metals [5]. This method has been widely used to study bulk samples of heavy rare earth metals and alloys, starting with the discovery of a 50-fold enhancement of the magnetic intensities in holmium at the L_3 edge [6]. Due to the smaller values of the moments, much less work has been published on the light rare earths Nd [7, 8] and Sm [3, 9]. However, the high beam intensities available from the new synchrotron radiation sources have made their study easier, as well as the study of rare earth thin films, going down to thicknesses of a few hundred ångströms [10]. The element selectivity of RXMS also allows one to study separately the magnetism of the different elements in rare earth superlattices [11, 12]. Moreover, the resonant process is shell selective [13], which in the case of rare earths can lead to a separate observation of the contributions of the 4f and 5d electrons to the magnetism [14]. Dipolar resonances at the $L_{2,3}$ edges of rare earths come from virtual electric multipolar transitions between the 2p core level and the 5d band, whereas quadrupolar resonances are related to $2p \rightarrow 4f$ transitions. The two types of resonance are observed at incident photon energies that usually differ by a few eV. For given incident and outgoing polarizations of the x-ray beam, dipolar and quadrupolar resonances have a different angular dependence, which can allow one to identify them [13–15]. A highly polarized incident beam and an efficient polarization analysis are thus decisive in the successful identification of the contributions from the different shells. A difficulty in magnetic x-ray scattering from thin films and superlattices arises from the high charge background: scattering from the substrate, structural superlattice peaks or finite thickness effects.... Polarization analysis presents the important property of removing most of this parasitic charge scattering background: whereas charge (Thomson) scattering does not rotate the incident polarization perpendicular to the scattering plane (σ-polarization), magnetic scattering also has a non-zero σ–π term that rotates the polarization into the scattering plane (π-polarization). In the σ–π-polarization channel, the charge background is reduced by several orders of magnitude [11].

Taking advantage of the above properties of the RXMS technique and of the high crystal quality available for rare earth samples prepared by molecular beam epitaxy (MBE) [16–22], we decided to revisit the magnetism of samarium and to extend the study to thin films and superlattices. The present work is devoted to an RXMS study of a 5000 Å thick (001) Sm film and of a [Sm (130 Å)/Y (105 Å)]$_{10}$ superlattice. The scope of the paper is as follows. Section 2 describes the preparation and characterization of the samples and gives the details of the RXMS experiments. Sections 3 and 4 are devoted to the results obtained from the pure Sm film and from the Sm/Y superlattice respectively. Our conclusions are presented in section 5.

2. Samples and experimental details

The samples were prepared by molecular beam epitaxy in a vacuum chamber with a base pressure of 4×10^{-11} Torr. Following the method proposed by Kwo *et al* [16], the (110) sapphire substrate was first covered by a 500 Å niobium buffer. Samarium and yttrium were then evaporated from an effusion cell and an electron gun respectively, and deposited (at 5 Å s^{-1}) onto the substrate kept at 280 °C. The samples were protected from oxidation

by a 500 Å thick Nb cap layer. The epitaxial relationships along the growth direction are $(110)Al_2O_3 \parallel (110)Nb \parallel (001)$ Sm and Y.

The RXMS experiments were performed at the BM28 beamline (the UK CRG beamline XMaS) at the European Synchrotron Radiation Facility. The beamline is located on the soft end of a bending magnet (critical energy 9.8 keV). The optics consists of a double Si(111) monochromator followed by a toroidal mirror. The vertical opening of the primary slits was reduced to 1.5 mm to improve the degree of horizontal linear polarization, with the loss of a factor 2 in the incident photon flux. The resulting degree of linear polarization was 95%, with a theoretical energy resolution of 2.1 eV at 6 keV. The samples were mounted in a closed-cycle refrigerator on the four-circle diffractometer, equipped with a polarization analyser on the detector arm. They were oriented with the $\boldsymbol{a}^*$- and $\boldsymbol{c}^*$-axes of the hexagonal structure in the vertical scattering plane. The measurements presented in sections 3 and 4 have all been performed in the σ–π-geometry, mostly to benefit from the low background. The polarization analyser crystal was a Cu(220) crystal with a mosaic spread of 0.28° and a peak reflectivity of 3.5% at 6.7 keV. At the L_3 edge of samarium, the Bragg angle of the Cu(220) reflection is 46.6°, close to the ideal value of 45°. The experiments were carried out by either scanning the wave-vector transfer $\boldsymbol{Q}$ through magnetic satellites at fixed photon energy along the $[0\,0\,l]$, $[0.25\,0\,l]$ and $[1\,0\,l]$ directions ('l-scans') or scanning the energy at fixed $\boldsymbol{Q}$ values ('energy scans').

Both samples were first characterized at room temperature by performing preliminary l-scans along $[0\,0\,l]$ and $[1\,0\,l]$ without polarization analysis. The 5000 Å film presents the 'Sm structure' with a c-parameter equal to the bulk value, $c = 26.21$ Å. The coherence length of the close-packed stacking is 830 ± 40 Å. The mosaic spread deduced from rocking curves is 0.13°. The samarium layers in the Sm/Y superlattice also present the Sm structure. The scan along $[0\,0\,l]$, figure 1, exhibits an average main Bragg peak surrounded by satellites showing the chemical superperiodicity (235 Å) of the sample. The structural coherence length in the growth direction is 450 ± 20 Å, i.e. the compact stacking is coherent over two Sm/Y bilayers. As expected, the main Bragg peak, which is an average of the Sm and Y contributions, is significantly shifted from the (0 0 9) Sm peak position. The mosaic spread is 0.27°. A scan performed along the $[1\,0\,l]$ direction shows peaks characteristic of the yttrium hcp structure and the samarium 'Sm structure' (figure 2). The full width at half maximum (FWHM) of these peaks as well as the lack of surrounding satellites demonstrate that the coherence of the hcp yttrium and of the 'Sm structure' samarium is confined to individual blocks. However, some extra peaks are observed at positions in the reciprocal space that correspond to a samarium dhcp structure. They are two orders of magnitude weaker than the 'Sm-structure' peaks, and this parasitic phase will be neglected in the present study. A more complete structural study of a series of superlattices will be the object of a different paper.

3. Magnetic ordering in the 5000 Å Sm film

3.1. Hexagonal sublattice

In the 5000 Å Sm layer, we investigated several magnetic reflections ((0 0 7.5), (0 0 16.5), (0 0 25.5) and (−1 0 15.5)) at 50 K at the samarium L_3 edge. The positions of these magnetic peaks in the reciprocal space correspond to a propagation vector $\tau = (0\,0\,1.5)$, consistent with previous results [2–4]. The energy scan at $\boldsymbol{Q} = (0\,0\,16.5)$ is shown in figure 3, together with the fluorescence measured away from any Bragg position. The solid vertical line indicates the position of the inflection point in the fluorescence. Three well resolved peaks are observed in the energy scan in figure 3(b). The lower energy peak has been identified as quadrupolar in

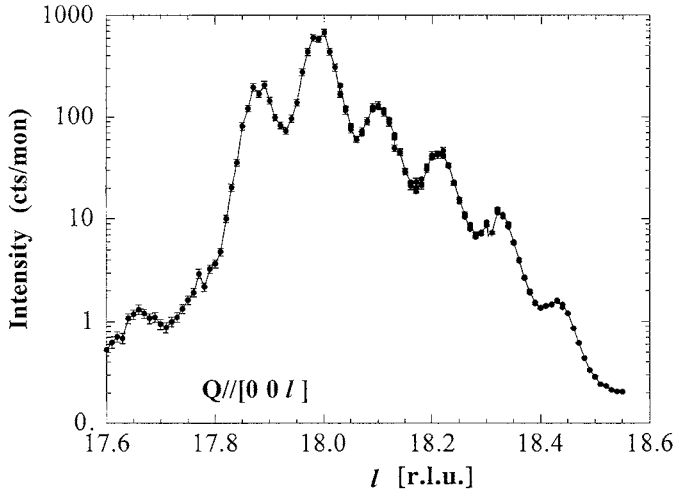

Figure 1. l-scan along the [0 0 l] direction, at $T = 300$ K for the Sm/Y superlattice.

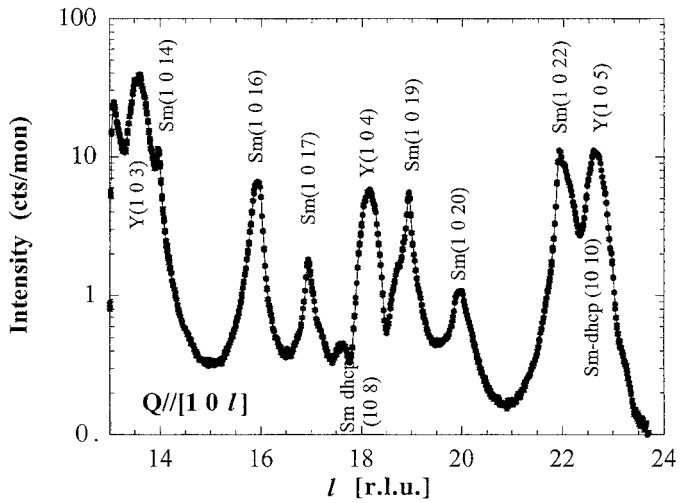

Figure 2. l-scan along the [1 0 l] direction, at $T = 300$ K for the Sm/Y superlattice.

origin, whereas the other two peaks, above the absorption edge, come from dipolar transitions and reflect the polarization of the 5d band [14]. The interpretation of the energy lineshape of the resonance involves reconsidering the classical atomic model [13] by including the band character of the 5d level [23].

l-scans have been performed at two different incident photon energies: measurements at 6.712 keV and 6.719 keV reflect the behaviours of the 4f and 5d moments respectively. As an example, figure 4 shows the l-scans around the (0 0 16.5) reflection. They both have the same width corresponding to a magnetic coherence length of 780 ± 50 Å, close to the structural coherence length in the c-direction.

The energy dependence of the resonance at the (0 0 16.5) position has also been measured at 105.5 K, close to T_N. The comparison of the integrated intensities (l-scans) at this temperature and at 50 K is shown in figure 5. The intensities at 105.5 K are 33 times smaller

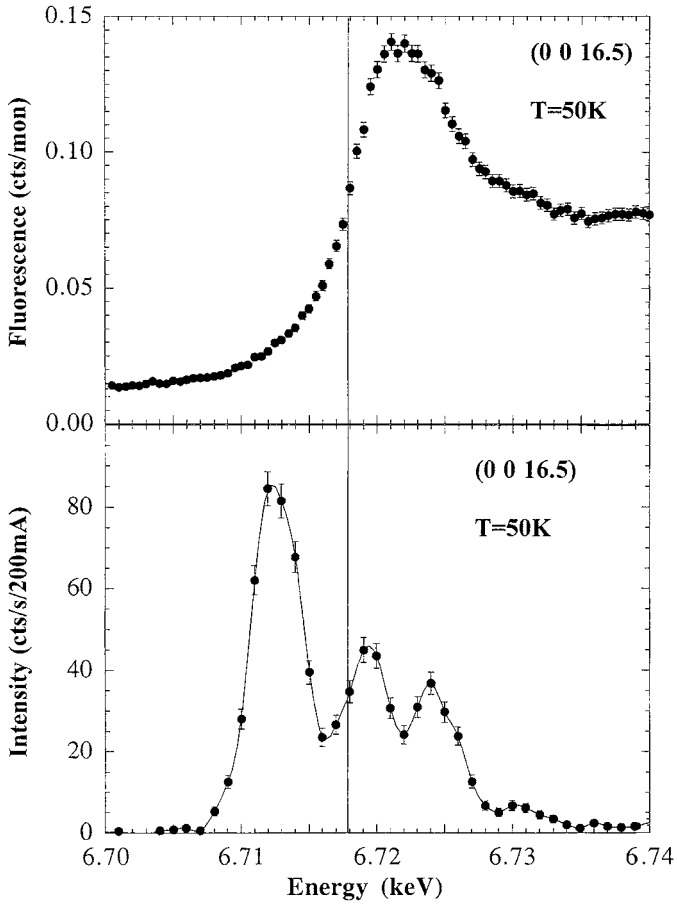

Figure 3. (a) Fluorescence around the Sm L_3 edge; (b) energy dependence of the peak intensity measured at the Sm (0 0 16.5) reflection in the 5000 Å film at $T = 50$ K. The vertical line corresponds to the L_3 edge of Sm.

than at 50 K, but the energy lineshape of the resonance is unchanged (figure 5). This shows a simultaneous polarization of the 4f and the 5d electrons even very close to T_N, in agreement with the RKKY model for long range magnetic order in rare earths.

3.2. Low temperature magnetic phase

At the lowest reachable temperature of 8 K, weak intensities (0.5 to 1 counts s^{-1}) were observed at positions in the reciprocal space corresponding to the periodicity of the long range magnetic order on the cubic sites: (0.25 0 9.25), (0.25 0 11.75), (0.25 0 15.25) and (0.25 0 18.25). The magnetic origin is confirmed by energy scans, as shown in figure 6 for the (0.25 0 15.25) reflection. The signal is however very low and its shape is different from the one collected around the hexagonal reflections: no dipolar contribution is observed above the edge. The weakness of the intensities at the quadrupolar resonance can be fully explained by geometrical considerations including the direction of the moments with respect to the direction and polarization of the incident and scattered beams. More surprising is the quasi-absence of a dipolar signal. If we consider for example the (0.25 0 15.25) reflection: the scattering geometry

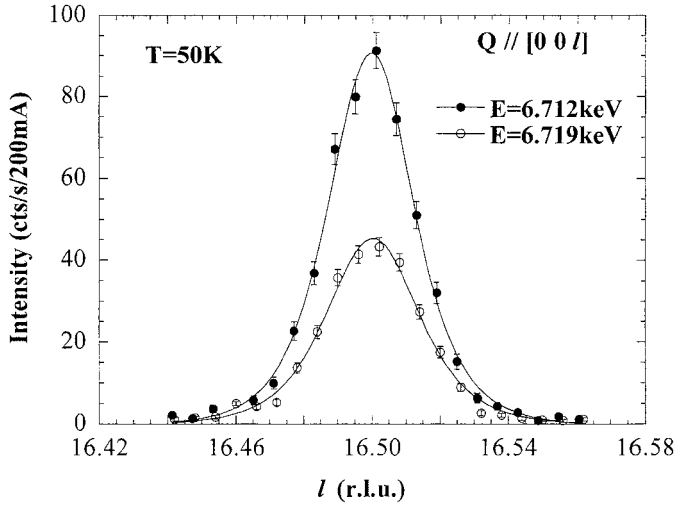

Figure 4. l-scans around the Sm (0 0 16.5) reflection in the 5000 Å film at $T = 50$ K. The incident photon energy was tuned to the energies of the quadrupolar (4f) resonance $E_{ph} = 6.712$ keV (full circles) and of the dipolar (5d) resonance $E_{ph} = 6.719$ keV (open circles). The lines are fits to a Gaussian line-shape.

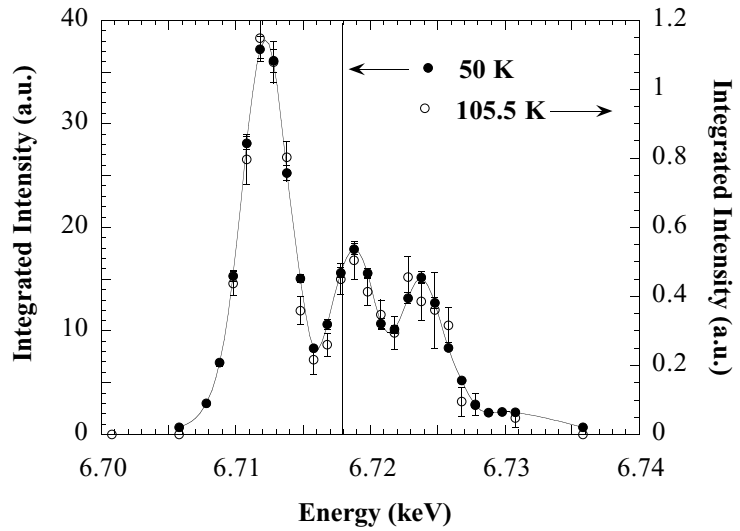

Figure 5. Energy dependence of the integrated intensity of the Sm (0 0 16.5) reflection in the 5000 Å film, at $T = 50$ K (full circles) and $T = 105.5$ K (open circles). The solid line is a guide for the eye. The vertical line corresponds to the position of the L_3 edge of Sm.

is very similar to the geometry at the (0 0 16.5) position (hexagonal sublattice) and a similar ratio between dipolar and quadrupolar amplitudes was expected. A deeper understanding of the resonant interaction and of the 5d magnetism will be needed to interpret this feature.

The study of the cubic phase was then performed at 6.712 keV, the energy of the quadrupolar (4f) resonance. l-scans were measured for all four observed reflections. Similarly to the hexagonal sublattice, the coherence length in the $\boldsymbol{c}$-direction of the long range magnetic

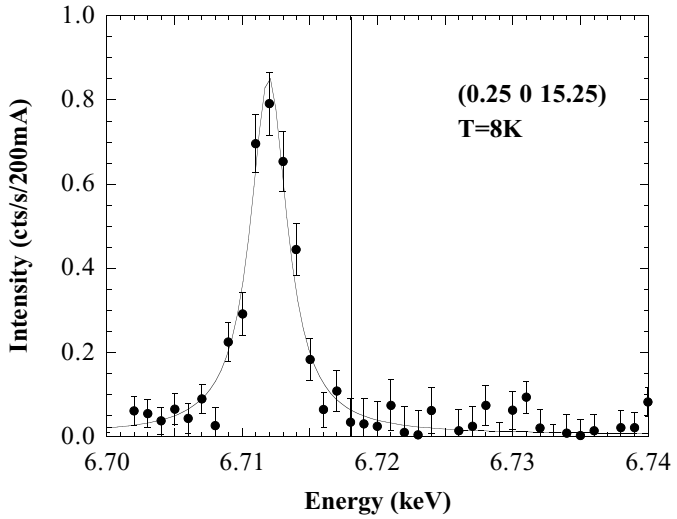

Figure 6. Energy dependence of the peak intensity measured at the Sm (0.25 0 15.25) reflection in the (001) Sm 5000 Å film, at $T = 8$ K around the L_3 edge of Sm. The solid line is a guide for the eye. The vertical line corresponds to the position of the L_3 edge of Sm.

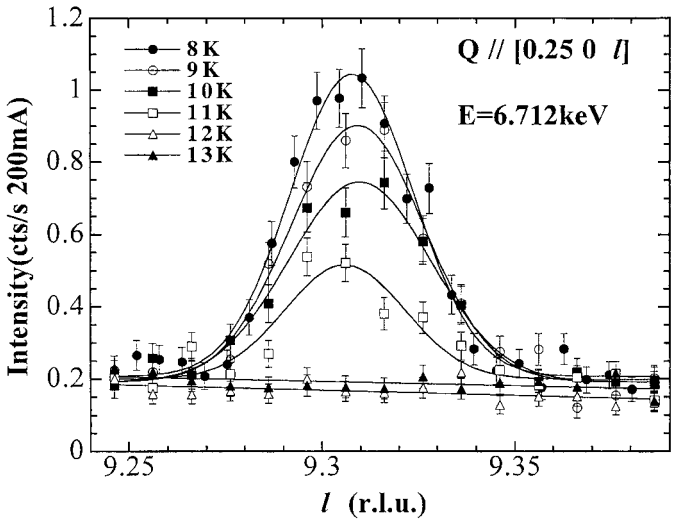

Figure 7. l-scans around the Sm (0.25 0 9.25) reflection in the (001) Sm 5000 Å film at different temperatures. The photon energy was tuned to $E_{ph} = 6.712$ keV. The solid lines are fits to a Gaussian line-shape. The peaks are shifted from the 9.25 position because the reference unit cell has been defined at room temperature.

order of the cubic sublattice is equal to the chemical coherence length. The temperature dependence of the strongest reflection is shown in figure 7. The resulting magnetic ordering temperature (=12 K) is close to the bulk value [2].

l-scans and corresponding energy scans have been performed at 8 K around the magnetic reflections from the hexagonal sublattice. The FWHM of the l-scans is the same as at 50 K: the magnetic ordering of the cubic sublattice has no influence on the coherence length of

the magnetic structure of the hexagonal sublattice. Moreover, the energy lineshape of the resonance is unchanged when the sample is cooled down below 12 K. We still observe the same quadrupolar and split dipolar contributions with the same relative intensities as at 50 K. The striking result is the lack of influence of the cubic site ordering on the polarization of the 5d band on the hexagonal sites: the projection of the polarization of the 5d band at the hexagonal sites is not modified by the establishment of long range order, i.e. a polarized coherent 5d wave, between the cubic planes.

4. Magnetic ordering in the (001) Sm/Y superlattice

We studied the (001) Sm (130 Å)/Y (105 Å) superlattice at the Sm L_3 edge. Unfortunately, the available energy range at the XMaS beamline (3–15 keV) does not allow a study of the yttrium layers by RXMS. At the Sm L_3 edge, we succeeded in extracting a magnetic contribution from the hexagonal sublattice of the samarium layers. We measured the (0 0 16.5) satellite at various temperatures. The weakness of the signals (less than 1 photon s^{-1} on a background higher than in the thick film, due to the superperiodicity and to the presence of yttrium) did not allow an accurate determination of the ordering temperature, which could only be estimated to be close to the bulk value. It was however impossible to extract any magnetic contribution from ordering of the cubic sublattice. Considering the weakness of the expected intensity ($= 0.1$ counts s^{-1}), we cannot know whether the sample temperature was low enough for long range order in the cubic sublattice to establish.

The magnetic coherence length deduced from the FWHM of l-scans is of the order of the thickness of one single samarium layer. Thus, similarly to the 'Sm-structure' crystallographic order, the long range magnetic order is confined in the individual Sm layers and does not propagate through the intermediate Y spacer layers. The same behaviour has already been reported in the case of Nd/Y superlattices [24], whereas Er/Y [18], Ho/Y [19], Gd/Y [22] and Dy/Y [17] show magnetic coupling of the rare earth layers across the non-magnetic layer. Other Sm/Y superlattices are under investigation to determine whether the large thickness of yttrium

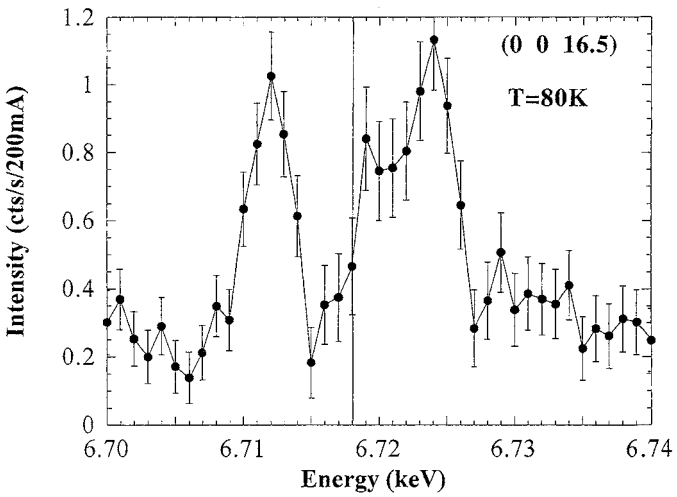

Figure 8. Energy dependence of the peak intensity (after background subtraction) measured at the Sm (0 0 16.5) reflection in the (001) Sm/Y superlattice, at $T = 80$ K around the L_3 edge of Sm. The vertical line corresponds to the L_3 edge of Sm.

films is responsible for this lack of coherence or if it is due to a more fundamental reason, such as differences between the Fermi surfaces of hcp yttrium and 'Sm-structure' samarium. The magnetic coherence being mediated by conduction electrons in both elements, similar Fermi surfaces may be necessary for a magnetic order to propagate coherently from one Sm layer to the next one.

The energy scan performed at the (0 0 16.5) reflection at 80 K (figure 8) is different from the thick film one (figure 3). It also presents three contributions: a peak located just below the L_3 edge energy and ascribed to a quadrupolar transition and two peaks on the high energy side attributed to dipolar transitions. The resonances are at the same energies as in the thick film, but the dipolar contribution is comparatively much stronger than in the film. Once again, a systematic study of superlattices with different Sm thicknesses is needed to check on the possible effect on the dipolar intensity that could be related to thin film behaviour or strain.

5. Conclusion

Samarium is a fascinating rare earth metal with complex crystallographic and magnetic structures. For the study of its magnetism on a microscopic scale, RXMS is a very good alternative to neutron scattering. We could benefit from the low background level offered by polarization analysis to study the magnetic order in the hexagonal sublattice in both our samples, as well as in the cubic sublattice in the thick film. The dipolar and quadrupolar resonances from samarium at the L_3 edge are clearly split in energy. The present study shows the advantage one can take of the shell selectivity of the technique, to study the 4f and 5d contributions to the magnetism separately. Long range magnetic order in rare earths is known to propagate through the 5d electrons (RKKY interaction). The study of the Sm thick film has shown that this is true even very close to T_N. We could also observe that the establishment of the long range magnetic order in the cubic sublattice does not influence the projection of the polarization of the 5d electrons at the hexagonal sites. Finally, the relative intensities of the quadrupolar and dipolar contribution are modified in the Sm/Y superlattice compared to the thick Sm film.

A systematic study of films and superlattices of different thicknesses is under way, to understand the thin film and/or strain effect on the energy line-shape of the resonance.

References

[1] Daane A H, Rundle R E, Smith H G and Spedding F H 1954 *Acta Crystallogr.* **7** 532
[2] Koelher W C and Moon R M 1972 *Phys. Rev. Lett.* **29** 1468
[3] Lee S L, Forgan E M, Shaikh S J, Tang C C, Stirling W G, Langridge S, Rollason A J, Costa M M R, Cooper M J, Zukowski E, Forsyth J B and Fort D 1993 *J. Magn. Magn. Mater.* **127** 145
[4] Dumesnil K, Dufour C, Mangin Ph, Brown J, Hennion M 1999 *Phys. Rev.* B **60** 10 743
[5] McMorrow D F, Gibbs D and Bohr J 1999 *Handbook on the Physics and Chemistry of Rare Earths* vol 26, ed K A Gschneidner (Amsterdam: Elsevier) p 1
[6] Gibbs D, Grübel G, Harshman D R, Isaacs E D, McWhan D B, Mills D and Vettier C 1991 *Phys. Rev.* B **43** 5663
Sutter S, Grübel G, Vettier C, de Bergevin F, Stunault A, Gibbs D and Giles C 1997 *Phys. Rev.* B **55** 954
[7] Watson D, Forgan E M, Nuttall W J, Stirling W G and Fort D 1996 *Phys. Rev.* B **53** 726
[8] Watson D, Nuttall W J, Forgan E M, Perry S C and Fort D 1998 *Phys. Rev.* B **57** R8095
[9] Watson D, Forgan E M, Stirling W G, Nuttall W J, Perry S C, Costa M M R and Fort D 1995 *J. Magn. Magn. Mater.* **140–144** 743
[10] Nuttall W J, Stunault A, Lidström E, Stirling W G, Barrett D, Longfield M J, Manix D, Ward R C C and Wells M R *CMMP'97* p 27 (abstract)
Weschke E, Schüssler-Langeheine C, Meier R, Kaindl G, Sutter C, Abernathy D and Grübel G *ESRF Scientific Highlights* 1996/1997

[11] Dumesnil K, Stunault A, Mangin Ph, Vettier C, Wermeille D, Bernhoeft N, Langridge S, Dufour C and Marchal G 1998 *Phys. Rev.* B **58** 3172
[12] Goff J P, Sarthour R S, McMorrow D F, Yakhou F, Stunault A, Vigliante A, Ward R C C and Wells M R 1999 *J. Phys.: Condens. Matter* **11** L139–L146
[13] Hannon J P, Trammell G T, Blume M and Gibbs D 1988 *Phys. Rev. Lett.* **61** 1245
Hannon J P, Trammell G T, Blume M and Gibbs D 1989 *Phys. Rev. Lett.* **62** 2644
[14] Stunault A, Vettier C, Bernhoeft N, de Bergevin D, Dufour C and Dumesnil K *SPIE Conf. Proc.* **3773** p 295
[15] Hill J P and McMorrow D F 1996 *Acta Crystallogr.* A **52** 236
[16] Kwo J, Hong M and Nakahara S 986 *Appl. Phys. Lett.* **46** 319
[17] Salamon M B, Sinha S, Rhyne J J, Cunningham J E, Erwin R W, Borchers J and Flynn C P 1986 *Phys. Rev. Lett.* **56** 259
[18] Borchers J A, Salamon M B, Erwin R W, Rhyne J J, Du R R and Flynn C P 1991 *Phys. Rev.* B **43** 3123
[19] McMorrow D F, Jehan D A, Cowley R A, Waddling P P S, Ward R C C, Wells M R, Hagmann N and Clausen K N 1993 *Europhys. Lett.* **23** 523
[20] Dumesnil K, Dufour C, Mangin Ph, Marchal G and Hennion M 1996 *Phys. Rev.* B **54** 6407
[21] Tsui F and Flynn C P 1993 *Phys. Rev. Lett.* **71** 1462
[22] Kwo J, Gyorgy E M, McWhan D B, Hong H, DiSalvo F J, Vettier C and Bower J E 1985 *Phys. Rev. Lett.* **55** 1402
[23] Langridge S, Paixão J A, Bernhoeft N, Vettier C, Lander G H, Gibbs D, Sørensen S A, Stunault A, Wermeille D and Talik E 1999 *Phys. Rev. Lett.* **82** 2187
[24] Everitt B A, Salamon M B, Borchers J A, Erwin R W, Rhyne J J, Park B J, O'Donavan K V, McMorrow D F and Flynn C P 1997 *Phys. Rev.* B **56** 5452